SILICA AEROGEL FOR THE MECHANICAL REINFORCEMENT OF THERMOSET EPOXY POLYMERS

N. H. Kim[1], H. S. Hwang[1], J. -Y. Lee [1], K. H. Choi[2], I. Park[1,*]
[1] Korea Packaging Center, Korea Institute of Industrial Technology (KITECH), Bucheonsi, Gyeonggido 421-742, Korea, [2] Green Chemistry and Engineering Department, Korea Institute of Industrial Technology (KITECH), Cheonansi, Chungnam, 331-825, Korea
* Corresponding author (inpark@kitech.re.kr)

Keywords*: nano composites, polymer-matrix composites, porosity/voids, mechanical properties*

1 Introduction

For the last two decades, numerous studies have been conducted to evaluate the synthesis and to characterize polymeric nanocomposites because of their excellent performance when compared to conventional composite materials [1]. Nano-composites usually consist of nanosized mineral particles dispersed into a polymeric matrix. Silica, titania and smectite clays have been widely applied for the reinforcement of polymeric materials [2-6].
Mesoporous forms of silica synthesized by supramolecular assembly are of interest due to their large surface areas, uniform framework structures and readily controlled pore diameters [7]. Mesostructured silicas show promise for use as reinforcing agents for several engineering polymer systems at relatively low particle loadings due to their high surface area and the favorable interfacial interactions that occur between the polymer and the silica surface [8-18]. Attempts to prepare nanocomposites using hexagonal MCM-41, cubic MCM-48 and hexagonal SBA-15 silicas with various types of polymers including polyimide [8], poly(3-trimethoxysily) propyl methacrylate [9], polyvinyl acetate [10], polymethyl methacrylate [7], Nylon 66 [11] and polypropylene [12] have been made. Recently, Pinnavaia et al. reported that rubbery and glassy epoxy mesocomposites produced from MSU-J silica (pore volume: 1.6 cm^3g^{-1}, pore size: 5.2 nm, S_{BET}: 964 m^2g^{-1}) and MSU-F silica (pore volume: 2.2 cm^3g^{-1}, pore size: 18.4 nm, S_{BET}: 393 m^2g^{-1}) exhibited enhanced tensile modulus, strength, toughness, and elongation-at-break when compared to the pure epoxy polymer [13-16]. These large-pore mesostructures are more likely to undergo pore filling by polymer chains without the need for organic modifiers or complicated processing conditions. Moreover, large pore mesoporous silicas with high framework pore volumes should provide polymer nanocomposites with improved homogeneity due to the low intrinsic density of the silica particles [13].
Silica aerogels are unique porous materials composed of more than 90% air and less than 10% solid silica in the form of highly cross-linked network structures, which results in low thermal conductivity, and a large surface area (500~1000 m^2g^{-1}), pore size (5~100 nm) and pore volume (1.5~4.5 cm^3g^{-1}) [18-20]. The pore structure of aerogels is comparable to that of large pore mesostructures. Therefore, aerogels that have an open-pore structure can be readily adapted to polymer nanocomposites as reinforcing agents. In the present study, we report mechanical reinforcement of thermoset epoxy polymer (both rubbery and glassy) nanocomposites using a silica aerogel as a reinforcing agent.

2 Experimental

2.1 Materials

Epoxy resin EPON828, a diglycidyl ether of bisphenol (Resolution Performance Products), was used to prepare epoxy-silica aerogel nanocomposites. The α,ω-diamine polypropylene oxide $H_2NCH(CH_3)CH_2[OCH_2CH(CH_3)]_xNH_2$ was obtained from Aldrich under the trade name Jeffamine D-2000 (x~33.1) or Jeffamine D-230 (x~2.6). To synthesize the silica aerogel, sodium silicate (Na_2O = 9~19%, SiO_2 = 28~38%, Duksan Co.) was used as a silica source and ETMS (Aldrich) was used as a surface modifier of the silica.

2.2 Preparation of silica aerogel

A silica hydrogel was prepared using sodium silicate as the starting material. The sodium silicate was diluted with deionized water (sodium silicate: deionized water (weight ratio) = 1: 3) and 1.0M aqueous HCl solution was used to modify the pH of the silica sol to 5. The obtained silica was then stirred for 1min, after which the sol suspension was aged until gelation occurred. To remove the sodium, the hydrogels were washed with deionized water three times, after which the silica hydrogel was collected. Next, butanol solution (pH adjusted to 2 by HCl solution) containing ETMS (5 wt% to the hydrogel) was added to the hydrogel. The mixture was then refluxed at 110℃ (~10h) until the pore water was exchanged with butanol. The water was then removed using a Dean-Stark trap. Finally, the ETMS-modified alcogel was dried at 130℃ for 3h in a vacuum oven.

2.3 Preparation of nanocomposites

To prepare the epoxy polymer nanocomposites, a pre-determined amount of the silica aerogel was added to the epoxy resin (EPON 828) and mixed at 50℃ for 10min. A stoichiometric amount of the Jeffamine D-2000 (or D-230) curing agent was then added to the mixture and mixed at 50℃ for another 10min. The resulting slurry was out-gassed under vacuum and transferred to a silicon mold. Pre-curing of the nanocomposite was conducted at 75℃ for 3h, followed by an additional 3h cure at 125℃ to complete the crosslinking.

2.4 Characterizations

A N_2 adsorption-desorption isotherm was obtained at 77.3 K on an ASAP 2420 volumetric adsorption analyzer. The silica aerogel was outgassed at 90°C for 30min, followed by 230°C for 3h. The microstructure and the morphology of the silica aerogel were then observed by scanning electron microscopy (SEM, JSM 6701F, INCA) and transmission electron microscopy (TEM, Hitachi H-7500). In addition, tensile measurements of individually molded samples were conducted at ambient temperature according to ASTM standard D-412 using a STM-10E, United Testing System. Dog-bone specimens used in the tensile testing were 20mm long in the narrow region, 2mm thick, and 3mm wide along the center of the casting. The dynamic mechanical properties were determined using a dynamic mechanical analyzer (TA instrument, DMA 2980). The sample was subjected to dual-cantilever bending with an amplitude of 0.2% at a frequency of 1Hz. The temperature was increased at a heating rate of 2°C/min in the range of 30°C to 150°C.

3. Results and Discussion

3.1 Morphology and microstructure of silica aerogel

A solvent exchange step is required during the synthesis of silica aerogels to dry the hydrogels. Hexane or alcohols with low surface tension have generally been used to exchange pore water even when a supercritical CO_2 drying tool is used to remove the organic solvent confined in the silica pores. A surface modification process is also necessary to induce hydrophobicity on the silica aerogel surface to avoid water adsorption. The hydrophobic aerogel can preserve its low thermal conductivity due to the absence of water in the pores. The hydrophobicity also plays an important role in maintaining good compatibility with hydrophobic polymer chains. In this study, a silica aerogel was synthesized via simultaneous solvent exchange and

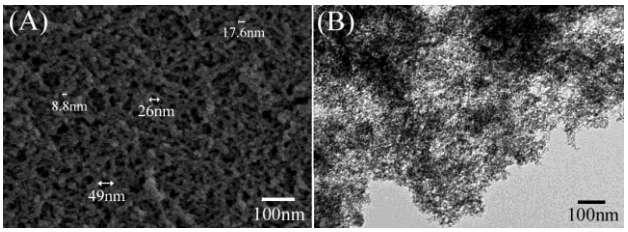

Fig.1. (A) SEM and (B) TEM images of the silica aerogel.

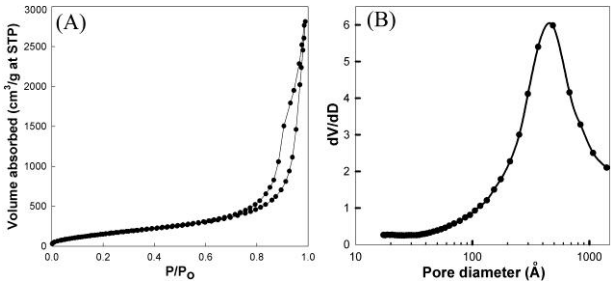

Fig.2. (A) Nitrogen adsorption-desorption isotherm of the silica aerogel and (B) the corresponding pore size distribution obtained from the adsorption branch.

surface modification in a butanol solution containing ETMS. Fig. 1. (A) shows the SEM morphology of the silica aerogel. The synthesized silica aerogel exhibited a porous network structure with 5–100 nm pores. A TEM micrograph of the obtained aerogel is shown in Fig. 1. (B). The silica aerogel exhibited a sponge-like mesostructure. The pore size observed in the TEM image was nearly identical to that of the SEM image in Fig. 1. A nitrogen absorption-desorption isotherm of the silica aerogel and the BJH pore size distribution obtained from the adsorption branch are presented in Fig. 2. The pore volume, BET surface area and pore size were 4.3 cm^3g^{-1}, 702 m^2g^{-1}, and 49 nm, respectively. The TEM image shown in Fig. 1 confirmed that the nanopore structure and pore size were in agreement with the value obtained from the nitrogen sorption isotherm.

3.2 Mechanical properties of rubbery epoxy-aerogel nanocomposites

The average pore size of the silica aerogel was large enough to allow both the epoxy resin and curing agent to readily fill the internal space of the mesostructured aerogel. Moreover, the pore structure of the aerogel was found to be open or 3-dimensional. Furthermore, modification of the silica surface with hydrophobic ETMS resulted in good compatibility with the hydrophobic epoxy chains. Due to the open pore structure and the hydrophobicity, the silica aerogel was readily dispersed in the epoxy matrix.

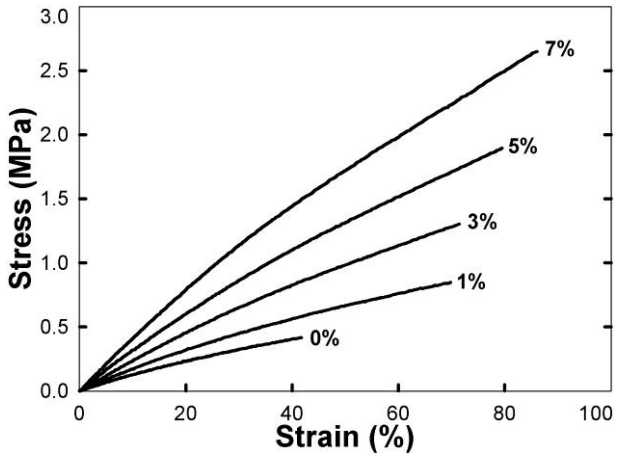

Fig.3. Stress-strain curves of pristine epoxy and rubbery epoxy-aerogel nanocomposites containing different aerogel loadings.

Tensile data describing the rubbery epoxy nanocomposites containing 1-7 wt% silica aerogel were obtained from load-displacement plots of dog-bone-shaped specimens. The stress-strain curves as a function of silica loading for the rubbery epoxy nanocomposites are provided in Fig. 3. The silica aerogel clearly provided composites with improved mechanical performance. The modulus, strength, elongation and toughness of the epoxy composites prepared from the silica aerogel generally increased as the silica loading increased (Fig. 4.).

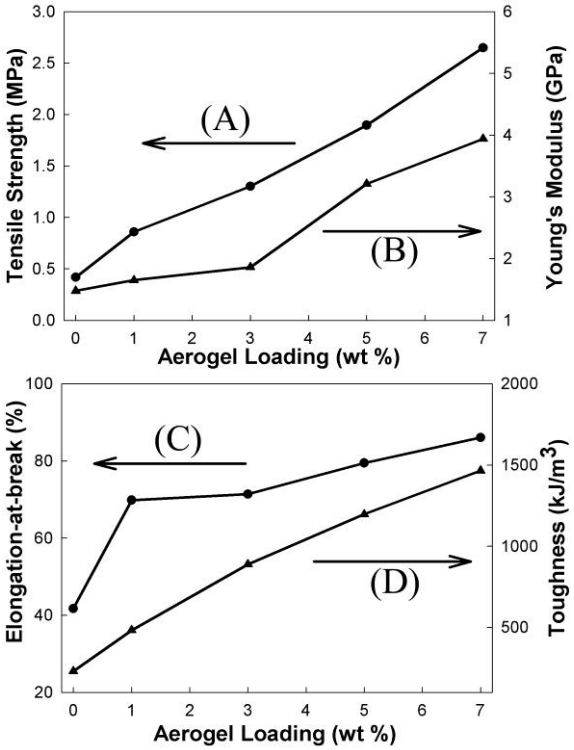

Fig.4. Loading dependence of the (A) tensile strength, (B) tensile modulus, (C) elongation at break and (D) toughness of rubbery epoxy nanocomposties prepared from silica.

Table 1. Tensile properties of pristine epoxy polymer and rubbery epoxy-aerogel nanocomposites.

Aerogel content wt%	Tensile Modulus MPa	Tensile Strength MPa	Toughness kJ m^{-3}	Elongation %
0	1.48	0.46	231	41.7
1	1.64	0.85	483	69.8
3	1.86	1.30	889	71.4
5	3.21	1.89	1197	79.5
7	3.94	2.55	1466	86.0

Table 1 summarizes the values of tensile properties.
The substantial improvement in the modulus, strength, and toughness achieved for the rubbery epoxy-aerogel nanocomposites in comparison to those of the pristine polymer were most likely a consequence of strong interfacial interactions and adhesion between the epoxy matrix and silica mesophase. The high surface area of the silica aerogel (702 m^2g^{-1}) likely facilitated such interfacial interactions. Similar improvements in tensile moduli, strength, and elongation-at-breaks have been observed for rubbery epoxy-mesoporous silica nanocomposites [13-16].The 2.7-fold increase in the modulus at 7% (w/w) aerogel loading that was observed in the present study was comparable to the 2.7-fold benefit in the modulus provided by MSU-F silica at an equivalent loading. However, the tensile strength and the elongation-at-break for the epoxy-aerogel nanocomposite (7 wt% loading) were not improved as much as for the previously reported MSU-F nanocomposite at the same silica loading.
In the case of mesostructured silica nanocomposites, the isotropic silica particles in the cured matrix can be partially aligned in the direction of the stress and further enhance tensile properties [13]. The similar particle morphology and alignment under applied stress may have caused the elongation-at-break to be 2.1-fold greater for the nanocomposites formed from the silica aerogel. For the nanocomposites formed from MSU-F, the elongation-at-break was 2.3-fold greater in response to the same 7% (w/w) loading. Unlike conventional reinforced composites, which sacrifice elasticity and toughness in exchange for benefits in modulus and strength, mesostructured silica and silica aerogels provide substantially improved tensile properties at relatively low particulate loadings.
The nanocomposites containing MSU-F silica with a higher pore volume (2.2 m^2g^{-1}) exhibited improved tensile properties when compared to the MSU-J nanocomposites (1.6 m^2g^{-1}) due to the higher volume fraction of MSU-F at the same silica loading [14]. The silica aerogel (4.3 m^2g^{-1}) contained a higher volume fraction than the MSU-F silica, but this did not increase its tensile properties. The silica framework of aerogels is known to be a pearl-necklace that consists of tangled strands of roughly spherical sol particles. Presumably, the silica framework of the MSU-F silica prepared through a supramolecular assembly pathway is more robust than that of the silica aerogel. Unlike the MSU-F silica, the silica aerogel was modified with hydrophobic ETMS, which enhanced the interfacial interaction between the silica surface and the epoxy chain. This hydrophobicity likely compensated for the weakness of the aerogel framework so that the epoxy-aerogel nanocomposites exhibited similar stiffness (modulus) to that of epoxy-MSU-F nanocomposites in response to the same silica loading. However, the improved interfacial interaction did not lead to improved strength or elongation-at-break. Therefore, the stiffness of the silica (stiffer than polymer) is a more important factor than that of its organic counterpart during the high elongation stage.

3.3 Thermal and mechanical properties of glassy epoxy-aerogel nanocomposites

Stress-strain curves for glassy epoxy-silica aerogel nanocomposites prepared from Epon 828 resin, Jeffamine D-230 curing agent and the silica aerogel as a reinforcing agent are shown in Fig. 5.

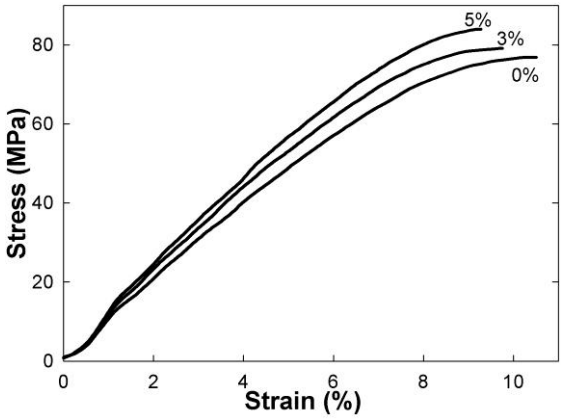

Fig.5. Comparison of stress-strain curves of pristine epoxy and epoxy-jeffamine D-230/aerogel nanocomposites containing different aerogel loadings.

Table 2. Tensile and thermal properties of pristine epoxy polymer and glassy epoxy-aerogel nanocomposites.

Aerogel content wt%	Tensile Modulus GPa	Tensile Strength MPa	Toughness MJ m^{-3}	Elongation %
0	1.08	76.9	47.1	10.5
3	1.19	79.1	48.6	9.8
5	1.24	83.9	50.3	9.3

The tensile data for different silica loadings are summarized in Table 2. The silica aerogel is an effective reinforcing agent for a glassy epoxy matrix. For example, at an aerogel loading of 5wt%, the tensile strength, modulus and toughness of the glassy matrix were increased by 9%, 15% and 7%, respectively, but the elongation-at-break decreased by 11%. The mechanical analysis demonstrated that the silica aerogels improved the stiffness and yield stress of the glassy epoxy. Similar improvements in tensile modulus and strength have been observed for glassy epoxy-mesoporous silica nanocomposites [15]. The 1.1-fold increase in modulus at 5% (w/w) aerogel loading observed in the present study was comparable to the 1.1-fold increase in modulus induced by MSU-J silica at an equivalent loading.

Generally, tensile properties of the relatively stiff glassy epoxy polymer were not significantly improved when compared to its rubbery counterpart, even if reinforcing agents such as smectite clays were used (unpublished data). It is noteworthy that the modulus of silica (~10 GPa) [14] has been shown to be much higher (>10,000 times) than that of the rubbery epoxy polymer. However, the difference in the modulus between silica and the glassy epoxy polymer was only three times; therefore, the 5 wt% silica-loaded samples exhibited only slightly improved mechanical performance, which was expected based on a simple rule of mixtures. The temperature dependence of the storage modulus (E′) and the tan δ of pure epoxy and glassy epoxy- aerogel nanocomposites are shown in Fig. 6. The nanocomposites had a higher storage modulus than that of the matrix. The storage modulus of the nanocomposites increased with filler content. The E′ values determined at 30℃ and 110℃ were compared for all samples and presented in Table 3. The E′ systematically increased with filler content in a fashion similar to that observed for the tensile tests. At 30°C, the E′ of the nanocomposite containing 5 wt% silica aerogel was 1.32 times greater than that of the pure epoxy. As expected and mentioned above, more improvement in modulus was observed in the range of rubbery states due to the large difference in modulus between the silica and the epoxy polymer. Fig. 6 also shows the temperature dependency of the tan δ for the pure epoxy and glassy epoxy-aerogel nanocomposites. The T_g values were determined at the maximum peaks of tan δ. As shown in Table 3, there was little or no shift in the T_g values at different silica loadings.

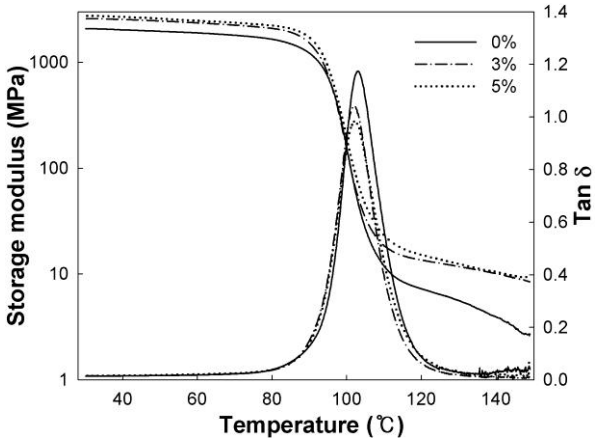

Fig.6. Temperature dependency of storage modulus and tan δ of pure epoxy (0%) and glassy epoxy-aerogel nanocomposites.

Table 3. Storage modulus (above and below T_g) and T_g values.

Aerogel content	Storage Modulus (MPa)		T_g ℃
wt%	30℃	110℃	
0	2083	11.9	103
3	2589	18.5	102
5	2746	23.3	102

4 Conclusions

Silca aerogel is an effective reinforcement agent for both rubbery and glassy epoxy polymers. In this study, reinforced thermoset epoxy nanocomposites were prepared from a silica aerogel with a surface area of 702 m^2g^{-1}, a pore size of 24.5 nm and a pore volume of 4.3 cm^3g^{-1}. The tensile modulus, tensile strength, elongation-at-break, and toughness of the rubbery nanocomposites were systematically enhanced by up to 2.7, 6.3, 2.1, and 6.3 times, respectively, at relatively low silica loading (≤7wt%). The 6.3-fold increase in tensile strength was higher than the improvement observed for mesocellular silica MSU-F/epoxy nanocomposites (4.9-fold increase) at the same silica loading. Moreover, the tensile properties and dynamic mechanical properties of the glassy nanocomposites were systematically enhanced at low silica loading (≤5wt%). Similar improvements in tensile modulus and strength have been observed for glassy epoxy-

mesoporous silica nanocomposites. The tensile modulus and the tensile strength showed a 1.1-fold increase for the glassy nanocomposites formed from silica aerogel, while nanocomposites formed from MSU-J showed increases in tensile modulus and strength of 1.1-fold at the same 5wt% loading.

Acknowledgement

This research was supported by a grant from the Fundamental R&D Program for Core Technology of Materials funded by the Ministry of Knowledge and Economy, Republic of Korea. NHK thanks So Hee Ko for valuable assistance in synthesis of the silica aerogel.

References

[1] G. Kickelbick "Concepts for the incorporation of inorganic building blocks into organic polymers on a nanoscale" *Progress in Polymer Science*, Vol. 28, 1, pp.83-114, 2003.

[2] E. P. Giannelis "Polymer Layered Silicate Nanocomposites" *Advaned Materials*, Vol. 8, 1, pp.29-35, 1996.

[3] P. C. LeBaron, Z. Wang , T. J. Pinnavaia "Polymer-layered silicate nanocomposites: an overview" *Applied Clay Science*, Vol. 15, 1-2, pp.11-29, 1999.

[4] V. M. Gun'ko, M. V. Borysenko, P. Pissis, A. Spanoudaki, N. Shinyashiki, I. Y.Sulim, T. V. Kulik, B. B. Palyanytsya, "Polydimethylsiloxane at the interfaces of fumed silica and zirconia/fumed silica" *Applied Surface Science* Vol. 253, 17, pp. 7143-7156, 2007.

[5] Y. H. Lai, M. C. Kuo, J. C. Huang, M. Chen "On the PEEK composites reinforced by surface-modified nano-silica" *Materials Science and Engineering: A* 2007;458(1-2):158-69.

[6] R. Bongiovanni, M. Sangermano, S. Ronchetti, A. Priola "Preparation and characterization of UV-cured epoxy nanocomposites based on o-montmorillonite modified with maleinized liquid polybutadienes" *Polymer* Vol. 48, 24, pp. 7000-7007. 2007

[7] M. T Run, S. Z. Wu, D.Y. Zhang, G. Wu "A polymer/mesoporous molecular sieve composite: Preparation, structure and properties" *Materials Chemistry and Physics* Vol. 105, 2-3, pp. 341-347. 2007.

[8] J. Lin, X. Wang "Novel low-κ polyimide/mesoporous silica composite films: Preparation, microstructure, and properties" *Polymer* Vol. 48, 1, pp.318-329. 2007.

[9] X. Ji, J. E. Hampsey, Q. Hu, J. He, Z. Yang, Y. Lu "Mesoporous silica-reinforced polymer nanocomposites" *Chemistry of Materials* Vol. 15, 19, pp. 3656-3662, 2003.

[10] J. He, Y. Shen, J. Yang, D. G. Evans, X. Duan "Nanocomposite structure based on silylated MCM-48 and poly (vinyl acetate)" *Chemistry of Materials* Vol. 15, 20, pp. 3894-3902, 2003.

[11] Y. Kojima, T. Matsuoka, H. Takahashi "Preparation of nylon 66/mesoporous molecular sieve composite under high pressure" *Journal of Applied Polymer Science* Vol. 74, 13, 3254-3258, 1999.

[12] N. Wang, M. Li, J. Zhang "Polymer-filled porous MCM-41: An effective means to design polymer-based nanocomposite" *Materials Letters* Vol. 59, 21, 2685-2688, 2005.

[13] I. Park, H. G. Peng, D. W. Gidley, S. Q. Xue, T. J. Pinnavaia "Epoxy−Silica mesocomposites with enhanced tensile properties and oxygen permeability" *Chemistry of Materials* Vol. 18, 3, pp. 650-656, 2006.

[14] I. Park, T. J. Pinnavaia "Mesocellular silica foam as an epoxy polymer reinforcing agent" *Advanced Functional Materials* Vol.17, 15, pp.2835-2841, 2007.

[15] J. Jiao, X. Sun, T. J. Pinnavaia "Mesostructured silica for the reinforcement and toughening of rubbery and glassy epoxy polymers" *Polymer* Vol. 50, 4, 983-989. 2009.

[16] J. Jiao, X. Sun, T. J. Pinnavaia "Reinforcement of a Rubbery Epoxy Polymer by Mesostructured Silica and Organosilica with Wormhole Framework Structures" *Advanced Functional Materials* Vol.18, 7, pp. 1067-1074,2008.

[17] F. A. Zhang, D. K. Lee, T. J. Pinnavaia, "Mesostructured silica for the reinforcement and toughening of rubbery and glassy epoxy polymers" Polymer Vol. 50, 20, pp. 4768-4774, 2009.

[18] A. P. Rao, A. V. Rao, G. M. Pajonk, "Hydrophobic and physical properties of the two step processed ambient pressure dried silica aerogels with various exchanging solvents" *Journal of Sol-Gel Science and Technology* Vol. 36, 3, pp. 285-292, 2005.

[19] S. D. Bhagat, A. V. Rao "Surface chemical modification of TEOS based silica aerogels synthesized by two step (acid–base) sol–gel process" *Applied Surface Science* Vol. 252, 12, pp. 4289-4297, 2006.

[20] D. Haranath, P. B. Wagh, G. M. Pajonk, A. V. Rao "Influence of sol-gel processing parameters on the ultrasonic sound velocities in silica aerogels" *Materials Research Bulletin* Vol. 32, 8, pp. 1079-1089, 1997.